Global and Planetary Change 142 (2016) 136–146

Contents lists available at ScienceDirect

Global and Planetary Change

journal homepage: www.elsevier.com/locate/gloplacha

The ELSA-Flood-Stack: A reconstruction from the laminated sediments of Eifel maar structures during the last 60 000 years

H. Brunck *, F. Sirocko, J. Albert

Institute for Geosciences, Johannes Gutenberg-University, J.-J. Becherweg 21, D-55128 Mainz, Germany

ARTICLE INFO

Article history:
Received 30 May 2015
Received in revised form 6 November 2015
Accepted 4 December 2015
Available online 4 January 2016

Keywords:
Flood frequency
Flood events
Eifel
Holocene
Late Pleistocene
Paleoclimate

ABSTRACT

This study reconstructs the main flood phases in central Europe from event layers in sediment cores from Holocene Eifel maar lakes and Pleistocene dry maar structures. These reconstructions are combined with recent gauge time-series to cover the entire precipitation extremes of the last 60 000 years. In general, Eifel maar sediments are perfectly suited for the preservation of event layers since the deep water in the maar lakes is seasonal anoxic and therefore, bioturbation is low. However, the preservation of annual lamination is only preserved in Holzmaar and Ulmener Maar; the other cores are dated by ^{14}C, magnetostratigraphy, tephra markers and ice core tuning. The cores were drilled in the Eifel region of central western Germany, which represents a climatic homogenous region from Belgium to Poland and all across Central Europe.

A total of 233 flood layers over 7.5 mm were detected in all analysed cores. The stratigraphic classification of the flood events follows the newly defined Landscape Evolution Zones (LEZ). The strongest events in the Holocene have occurred during LEZ 1 (0–6000 b2k) in the years 658, 2800 and 4100 b2k. Flood layers in the LEZ 2 (6000–10 500 b2k) are not as frequent as during the LEZ 1, nevertheless, the floods cluster between 6000 and 6500 b2k. Twenty flood layers are found in the LEZ 3 (10 500–14 700 b2k); 11 in LEZ 4 (14 700–21 000 b2k); 15 in LEZ 5 (21 000–28 500 b2k); 34 in LEZ 6 (28 500–36 500 b2k); 8 in LEZ 7 (36 500–49 000 b2k); zero in LEZ 8 (49 000–55 000 b2k) and LEZ 9 (55 000–60 000 b2k). The maximum flood phases during the Pleistocene are at 11 500–17 500 (late glacial and Younger Dryas), 23 000–24 000 (before Greenland Interstadial (GI) 2), 29 000–35 000 (especially between GI 5 and 4) and 44 000–44 500 b2k (transition from GI 12 to 11).

The variations in flood dynamics are climatically driven and mainly associated with climate transitions and colder periods, combined with light vegetation. It turns out that low vegetation coverage related to both Greenland Stadial phases and anthropogenic impacts since late Holocene is the main cause for the development of flood layers in maar sediments. The precipitation itself, plays only a secondary role. This interpretation is based on the current climate understanding of cold phases and several studies of fluvial erosion related to vegetation coverage.

© 2016 Elsevier B.V. All rights reserved.

1. Introduction

The weather of the next decades will most likely undergo an intensification of weather extremes. Prognostic models have highlighted an intensification of prolonged summer droughts and precipitation maxima combined with a higher risk of flash floods in creeks and rivers (IPCC report 2014 and 2007; Jacob et al., 2007). Lacustrine sediments are very sensitive to natural and anthropogenic environmental changes. Thus, lake sediments are excellent climate archives and have been used for reconstructions of vegetation, water temperature, environment, volcanic activity, climate and quite recently, for precipitation and flood events (e.g. Wessels, 1998; Macklin et al., 2006; Moreno et al., 2008; Zielhofer et al., 2008; Storen et al., 2010; Wilhelm et al., 2012a, 2012b, Swierczynski et al., 2013; Wirth et al., 2013; Kämpf et al., 2014).

Lakes that are used for the Holocene reconstructions are numerous in the landscape of central Europe. However, lakes that have the potential to reconstruct the climate conditions between 10 000 and 60 000 b2k in central Germany are restricted to Eifel maar structures. The Eifel region is characterized by a climatic homogenous area from Belgium to Poland and all across Central Europe (Wernli and Pfahl, 2009). Other suitable locations are in central France (Ampel et al., 2008; Wohlfarth et al., 2008) or southern Italy (Brauer et al., 2000, 2001), and thus in regions with another climate forcing. River sediments are a complicated and incomplete archive, due to the fact that flood event layers are separated by erosion from the normal sedimentation (Brakenridge et al., 1988; Macklin, 1999; Thorndycraft et al., 2005). Small basins, like maars, with long water residence time and anoxic bottom water are better suited to preserve a complete flood archive, if they are fed by small creeks. The suspension layers can be distinguished from

* Corresponding author.
E-mail addresses: heiko.brunck@gmail.com (H. Brunck), sirocko@uni-mainz.de (F. Sirocko), albertj@students.uni-mainz.de (J. Albert).

http://dx.doi.org/10.1016/j.gloplacha.2015.12.003
0921-8181/© 2016 Elsevier B.V. All rights reserved.

background sedimentation and seismites macroscopically or in thin sections (Marco et al., 1996; Moreno et al., 2008). Further sedimentological (e.g. grain size analysis) and geochemical (e.g. μ-XRF analysis) studies help to differentiate between flood layers, turbidites and slumps (Sturm et al., 1995; Mulder et al., 2003; Wirth et al., 2011). Accordingly, the Eifel maar lakes are the only location in central Europe that allows one to generate a long time series with event resolution (Sirocko et al., 2013).

The maar lakes and the dry maar structures of the Eifel region have been systematically cored since 1998 by the ELSA Project (Eifel Laminated Sediment Archive; http://www.elsa.geowissenschaften.uni-mainz.de) of the Institute for Geoscience, Johannes Gutenberg University Mainz, Germany. In this study, the maar structures of Holzmaar, Ulmener Maar, Schalkenmehrener Maar and Aueler Maar are used to reconstruct the flood history of the last 60 000 years. In contrast, studies on the average precipitation are better done in the closed/semiclosed basins of Gemündener Maar or Dehner Maar, where terraces document past lake levels (Sirocko et al., 2013). So far, the flood history of the last 60 000 years is increasingly studied in the Holocene, the time before 10 000 years is still completely unknown.

The key objectives of this study are: (1) to develop a high resolution long time flood frequency record for central Europe; (2) to analyse the relationship between flood activity and a) climate, b) precipitation and c) vegetation; and (3) to study the last 60 000 years with respect to the interlacing of flood layers and predominant climatic and anthropogenic development.

2. Coring sites

Four sediment cores (from three Holocene maar lakes and one Pleistocene dry maar structure) are used to reconstruct the flood activity in the Eifel for the last 60 000 years (Fig. 1).

2.1. Schalkenmehrener Maar

Lake Schalkenmehrener Maar is part of the Dauner Maare. It has a diameter of 528 m, an average depth of 14.5 m and a maximum depth of 21 m (Scharf and Oehms, 1992). With a lake surface of 219 000 m^2, it is one of the larger maar lakes of the Eifel. It has no large inflow or outflow stream. However, it is connected to a flanking dry maar, which is filled with sediment and peat since the middle Holocene (Straka, 1975) and drained since Roman times (Sirocko, 2009). Accordingly, Schalkenmehren is well suited to monitor the post-Roman landscape evolution. The freeze core SM$_{f2}$ (Fig. 1) was used for the flood event reconstruction depicting the last 1000 years; in particular the medieval landscape history.

2.2. Holzmaar

The most investigated maar of the Eifel is the Holzmaar. The stratigraphy for this maar includes annual varve counting, which was constrained using ^{14}C-dating (Brauer, 1994; Hajdas et al., 1995; Zolitschka, 1998, and Brauer et al., 1999a, 1999b). Holzmaar has a diameter of 272 m and a maximum depth of 20 m (Scharf and Oehms, 1992). It also has the smallest water volume of all maar lakes in the Eifel. The Sammetbach flows from the west into the maar. Just a few metres further south it flows out again. The small size of the maar and the direct inflow by the Sammetbach cause a relative high sedimentation rate (10 m Holocene). Persistent low deep water oxygenation led to the formation of countable varves throughout the entire Holocene (Sirocko et al., 2016–in this volume).

2.3. Ulmener Maar

The Ulmener Maar is slightly smaller than the Holzmaar with a diameter of 265 m (Scharf and Oehms, 1992). It is the smallest and youngest maar in the Eifel (about 11 000 b2k). However, it is also one of the deepest with a maximum depth of 39 m (Scharf and Oehms, 1992). The Ulmener Maar has the largest catchment area of the three analysed Holocene maars. Up to the pre-Roman times flood sediments were flushed from the Dellbach into the maar. Nowadays, the Dellbach flows west of the maar and had no contact to it since the founding of the city Ulmen. Consequently, the Ulmener Maar can only be applied to reconstruct the pre-Roman flood history. Flood layers in the core UM2 have partly whitish colours, which correspond well to silt and clay sediments of Devonian age (Eckfeld and Reudelsterz layers) in the western catchment area of the maar. Pollen and botanical macroremains reveal that the region around the maar is anthropogenically modified since 5700 b2k (3700 BC) (Sirocko, 2009). Nevertheless, the Ulmener Maar is certainly the best suited for the early Holocene flood reconstruction and has a higher sedimentation rate than that of Holzmaar.

2.4. Auel dry maar

The silted up basin Auel is one of the largest dry maar structures of the Eifel with a diameter of 1325 m. The modern Tiefer Bach flows through the maar centre and leaves the dry maar again at the opposite side. This river has a large catchment area of 12.187 km^2 and a total length of 9.4 km (Water management administration Rhineland-

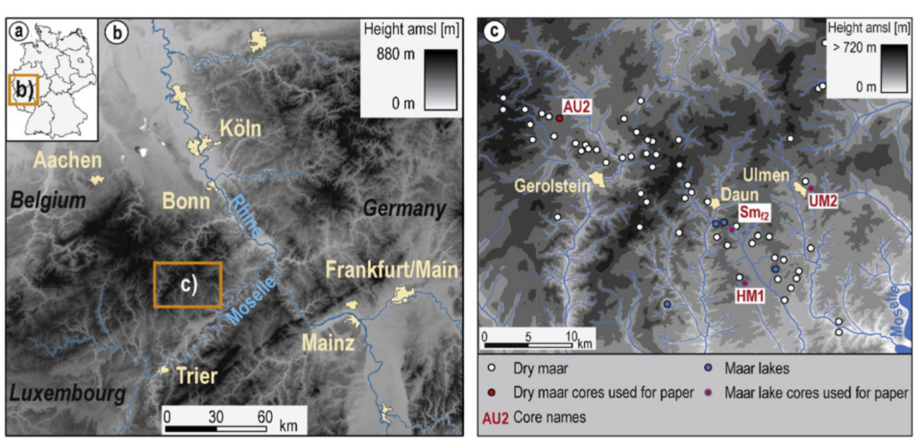

Fig. 1. a) Outline map of Germany. b) Digital terrain model West Germany with the drainage system c) Digital terrain model of the Eifel with the maar locations after Büchel (1993), the drainage system and the core positions: SM$_{f2}$ (Gauß-Krüger-Koordinatensystem Zone 2 (GK-System) 2,561,310/5,559,585); HM1 (GK-System 2,562,900/5,554,030); UM2 (GK-System 2,570,165/5,564,270) and AU2 (GK-System 2,542,455/5,572,017).

Palatinate: German river code 266,374). The core AU2 from the centre of the maar is 123 m long and covers the time from the Laacher See eruption (see also Förster & Sirocko, 2016–in this volume) back to 60 000 b2k (Fig. 2). The average sedimentation rate of dry maar lake Auel is with 2 mm/a the highest of all Eifel maar structures, due to the abundant fluvial input. Therefore, the largest flood events and associated suspension injections are nicely visible in the sediment. Additionally, the fluvial inflow also leads to a high amount of botanical macroremains. Frequent Ranunculaceae seeds are used for four new ^{14}C dates, which are measured between 18 340 and 21 865 b2k (see Fig. 19 in Sirocko et al., 2016–in this volume). Carbon maxima are visible for all Greenland interstadials, which are used to fine-tune the ^{14}C stratigraphy to the established Greenland ice core chronology (Svensson et al., 2008).

3. Stratigraphy

An integrated Age–Depth model for all ELSA cores was developed by using 9 different dating methods and sedimentological, palaeobotanical and geochemical data from 18 Eifel sediment cores (Sirocko et al., 2013). Based on this stratigraphical concept, tephra correlation and several new ^{14}C dates have improved the stratigraphy and leads to a classification of LEZ (Sirocko et al., 2016–in this volume). The LEZ reconstruct the vegetation and the climate change mostly based on macroremains and pollen since 60 000 b2k (Sirocko et al., 2016–in this volume). The stratigraphy and the LEZ classification are assumed on a one-to-one basis to discuss the flood event succession concerning environmental changes. The specific sedimentation conditions of Auel explain the unique possibility to detect all 17 GI in the total carbon concentration of this dry maar. In a final step, the time series of C_{total} was tuned to the Greenland ice core chronology GICC05 (Svensson et al., 2008) to link the central European landscape evolution directly to the Greenland climate curve (Sirocko et al., 2016–in this volume).The allocation of the core material to all Greenland Interstadials and Stadials (defined after Andersen et al., 2006) enables the exact climatic interpretation of the flood frequency.

In order to extend the flood record to the present, daily gauge values from the Rhine, Moselle and several Eifel rivers (Ahr, Kyll and Prüm) were analysed. Due to the fact that sediment cores are disturbed from human impact in all maar sites of the Eifel for the last decades, the strongest flood events since 180 b2k (1820 AD) were identified from the historical values. The correlation between the gauge analysis and the freeze core SM_{f2} is carried out with the flood events 118 and 155 b2k (AD 1882 and 1845) (Fig. 3). The millennium flood 658 b2k (1342 AD) was used for the transition from the freeze core SM_{f2} to the two Holocene cores (Bork et al., 1998). Additionally, the flood event 2800 b2k (BC 800/ Sirocko et al., 2013) and the Ulmener Maar Tephra (11 000 b2k/ Zolitschka et al., 1995) are applied as time markers between the cores HM1 and UM2. The Holocene core HM1 is correlated to the core AU2 through the Laacher See Tephra (LST) (12 900 b2k; Brauer et al., 1999b) (Figs. 2 and 3).

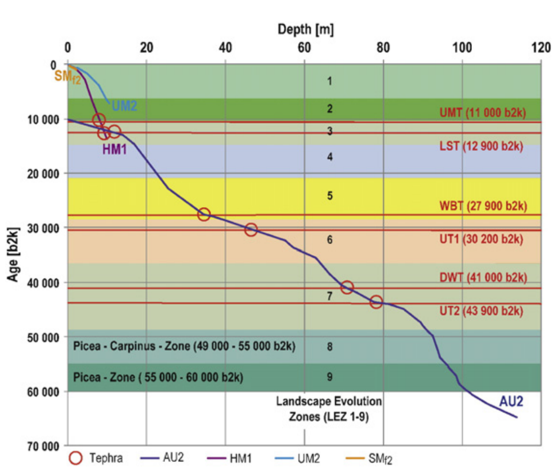

Fig. 2. Age–Depth model of the cores SM_{f2}, UM2, HM1 and AU2. The LEZ subdivisions 1–9 are colour-coded. Visible tephra layers are represented by red lines and marked with red circles in each core.

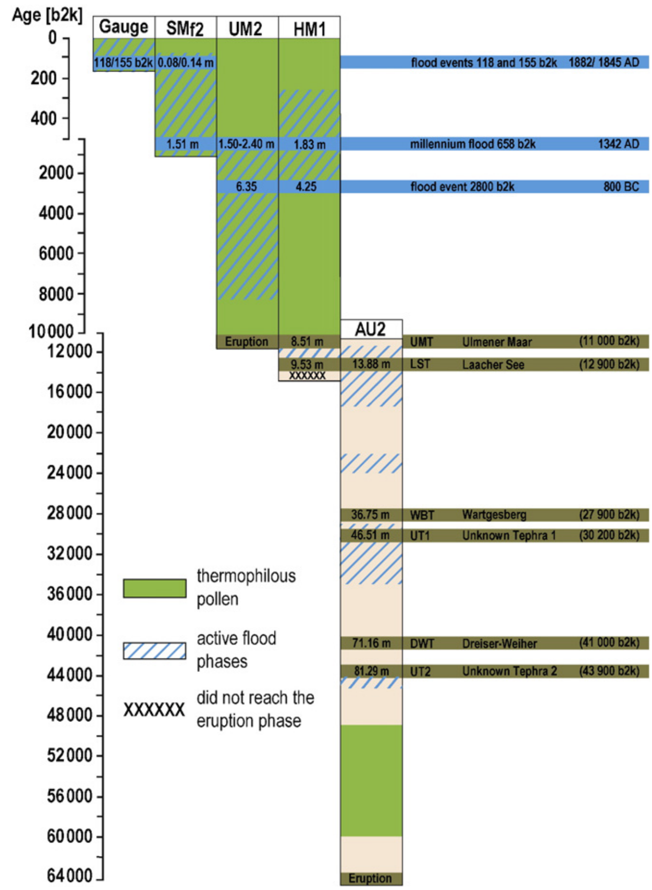

Fig. 3. Time series with transition points between the gauge analysis and the cores SM_{f2}, UM2, HM1 and AU2. In each core the transition points and all tephra layers are marked with their exact depth. The green highlighted parts of the cores represent time periods with thermophilous pollen (Sirocko et al., 2016–in this volume) and the hatched blue parts stands for active flood phases (Fig. 7).

4. Material and method

Four sediment cores were visually and lithologically examined to identify flood layers over 7.5 mm thickness. Some flood layers are several cm thick and clearly visible by the eye (Figs. 6 and 7). Others are mm thick and were petrographically studied in 10 cm long thin sections under an Olympus U-TTBI microscope to distinguish them from distal turbidites and distal slumps. Due to the different catchment areas and time relations of the maars, the normalised flood index was calculated by the number of flood layers per millennium divided by the maximal number of flood layers per millennium in each core.

The reconstructed time series was aligned with meteorological precipitation data and historically documented flood events. The historical record from Cologne (Municipal Drainage Operations of Cologne, Flood Protection Centre. www.steb-koeln.de, 18.02.2016) was used as reference system since 180 b2k (AD 1820). An extreme value analysis was applied to combine the daily gauge values from the Rhine and Eifel rivers to the core SM_{f2} (Dyck and Peschke, 1995). Thus, it was possible to extend the flood time series to recent years.

The core event sections were scanned for selected elements at 1 mm resolution using the X-ray fluorescence scanner Eagle III

(Röntgenanalytik Meßtechnik GmbH, Germany) of the University of Mainz (Germany). The major elements (NA, Mg, Al, Si, P, S, K, Ca, Ti, Mn, and Fe) as well as trace elements (Ni, Cu, Zn and Sr) were measured on 10 cm long resin impregnated samples with the μ-XRF (Fig. 4).

The particle analysis method RADIUS — Rapid Particle Analysis of digital Images by ultra-high-resolution scanning of thin sections (for details see Seelos and Sirocko, 2005), was used to analyse and identify the different sediment structures and events in the drilling cores of the ELSA archive (Sirocko et al., 2005) (Figs. 4 and 5).

5. Flood Layer — a definition

Flood Layers indicate fluvial inflow due to singular or repeating heavy rain events. The intensified sediment input is on one hand attributable to increased rainfall in the catchment area of the maar and on the other hand a combination of wind and wave erosion along the lakeside (Sturm et al., 1995; Mulder et al., 2003). During this process, mostly detrital minerogenic particles and terrestrial organic material are transported into the lake (Mulder et al., 2003; Wirth et al., 2011). Coarse-grained material deposits gravitationally on the slope and does not reach the position in the central maar basin where the ELSA cores are taken. During and immediately after heavy rain events, material stored in creeks and slopes are eroded and transported into the maar. Our field observations during three rain events and collected water samples in Schalkenmehren showed two major points: 1) increased fluvial transport of plant debris, wood remains and sand into the maar. 2) fine clastic and biogenic particles are transported within 2 h after the suspension event into the maar centre and settle to the ground. The final deposition of the finest particles occurs several days after the event (Moschen, 2004). Thus, the mm to cm thick flood events are usually completed by a clay layer, or "clay cap" (Schlolaut et al., 2014). The strongest flood events last over several days and result in a complex pattern of particle size and density as a consequence of variable sink rates of the particles. This causes a discontinuous grain size gradient within the flood layer. Therefore, the occurrence of several grain size maxima over the entire flood layer thickness is a key characteristic against turbidites and slumps (Sturm et al., 1995 and Anselmetti et al., 2009) (Figs. 4a and 5).

A turbidite is a singular event that leads to segregation and rearrangement of the entire carried sediment package (Bouma, 1987; Sturm et al., 1995). Such an event remobilizes unconsolidated and water-saturated particles, by the destabilization of the grain structure or pore water overpressure (Sirocko and Dietrich, 2009). The particles then segregate and flow to the maar bottom in a turbulent suspension layer. The fine-grained components remain in a suspension cloud, while denser and heavier material accumulates quickly on the ground or slide down the slope (Mulder and Alexander, 2001; Sirocko and Dietrich, 2009). The deposits extend over the entire ground and due to decreasing transport energy of the turbidity current, large and heavy particles settle first. The lighter and smaller particles remain essentially longer in suspension, therefore, deposited sediments are continuously graded (Walker and Mutti, 1973; Bouma, 1987; Schnellmann et al., 2005). Thus, turbidite sediments have a widespread grain size distribution and moderate sorting. In contrast to flood events, coarse particles are restricted to the base layer (Figs. 4b and 5).

Slumps are characterized by missing segregation of the sediment packages (Nardin, 1979). These packages move as a whole block down the slope and can be folded in a large scale from dm to m (see Suppl. 1, modified after Sirocko and Dietrich, 2009). Slumps are expressed by bent and tilted layers in the core; completely mixed slumps can be identified by the typical mottled appearance (Suppl. 1). Since slumps are triggered at the slope near the lakefront, all particle sizes and sediment colorations are present. Furthermore, slumps can also be detected in the particle size analysis by a very poor sorting and extreme changes of grain sizes (Fig. 4c).

6. Results: The ELSA-Flood-Stack

Flood events recorded by the gauge extreme value analysis identify the years 5 b2k (AD 1995), 7 b2k (AD 1993), 12 b2k (AD 1988), 52 b2k (AD 1948), 74 b2k (AD 1926), 80 b2k (AD 1920), 118 b2k (AD 1882) and 155 b2k (AD 1845) as the strongest floods since 180 b2k (AD 1820) (Table 1 and Fig. 8) (Federal Waterways and Shipping Administration, 2015). This is consistent with historical documents from Cologne (Municipal Drainage Operations of Cologne, Flood Protection Centre. www.steb-koeln.de, 18.02.2016). The flood events 118 b2k (AD 1882) and 155 b2k (AD 1845) are observed in the gauge analysis and can be correlated to the core SM_{f2} (Fig. 3). The varve counting of core SM_{f2} was tuned to these two flood layers (Table 1 and Fig. 6).

A combination of the cores SM_{f2}, HM1 and UM2 represents the Holocene. A total of 109 flood layers were detected in the LEZ 1 (0–6000 b2k; anthropogenic forest), with a clear maximum in the medieval and Roman sections of the cores. The strongest flood events are reconstructed for the years 658, 2800 and 4100 b2k (AD 1342, 800 and 2100 BC) (Table 1 and Fig. 8). The most pronounced flood was the St. Mary Magdalene's millennium flood in July 658 b2k (AD 1342) (Bork et al., 1998). This flood layer is unusually thick and contains a large amount of plant remains, which indicate the tremendous event strength. The millennium flood is visible in all maars and is therefore a

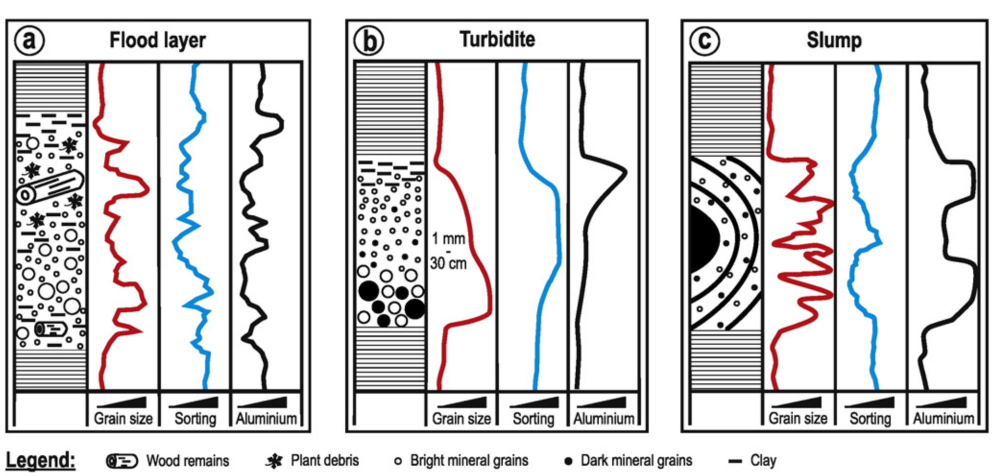

Fig. 4. a) Pattern of an idealized flood layer for the grain size, the sorting and the aluminium content. At the end of the flood layer the "clay cap" is visible. b) Pattern of an idealized turbidite for the grain size, the sorting and the aluminium content. c) Pattern of an idealized slump for the grain size, the sorting and the aluminium content.

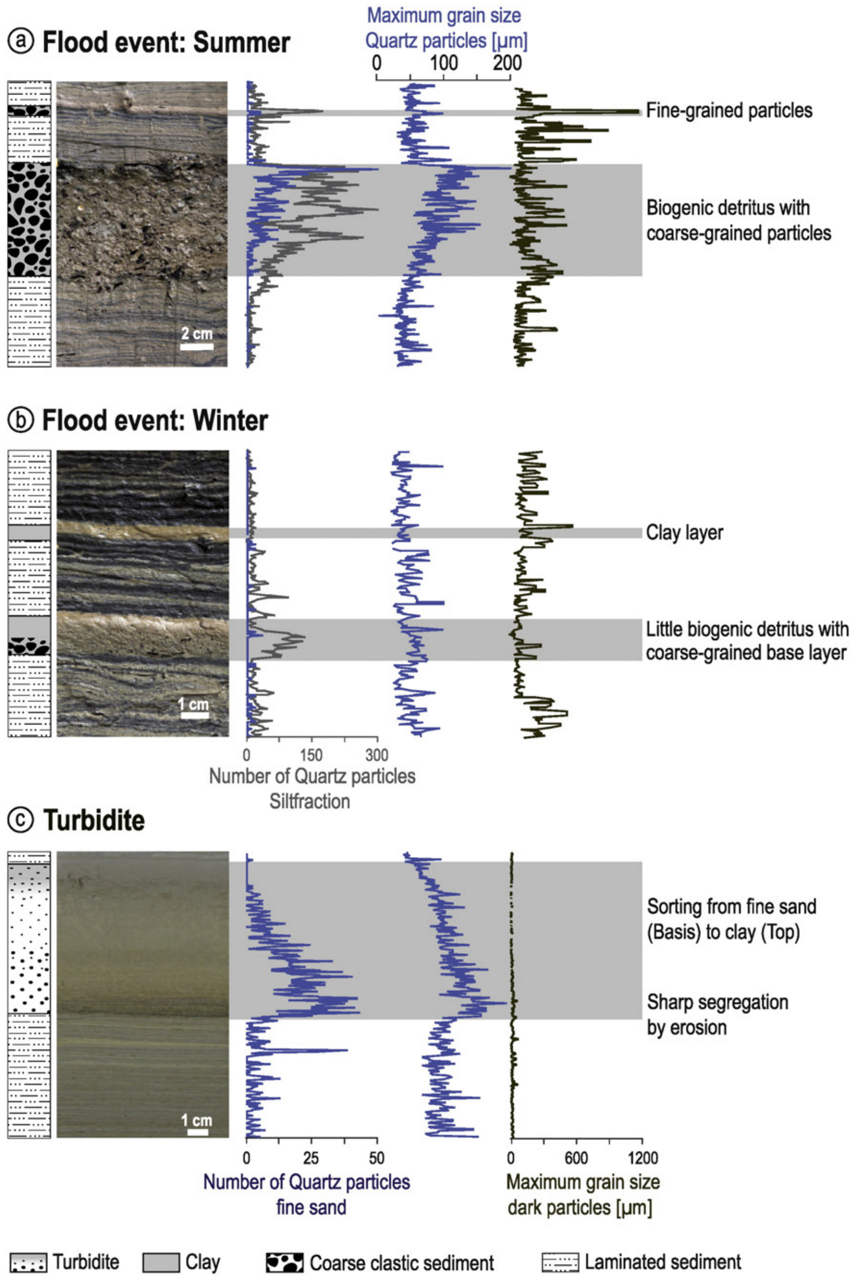

Fig. 5. Summer suspension layer (a), winter suspension layer (b) and Turbidite (c). Summer and winter suspension layers differ mainly in the content of biogenic detritus. In contrast, a turbidite is characterized by continuous grading of particle sizes. Modified after Sirocko and Dietrich (2009).

distinct time and correlation marker. Another major hydrological event is dated to approximately 2800 b2k (800 BC) in the cores HM1 and UM2. The layers include a large amount of reworked sediment and are thus difficult to date. Nevertheless, the flood layer is recognizable in all Holocene cores and can be used as a second time marker.

Flood events in LEZ 2 (6000–10 500 b2k; natural broadleaf forest) are not clearly visible in Holzmaar or Schalkenmehrener Maar. They become visible only in LEZ 1, when humans cultivated the landscape. However, 34 flood events are recognizable in the Ulmen Maar from 8500 to 6000 b2k (Gronenborn and Sirocko, 2009) (Table 1 and Fig. 8). They seem to cluster slightly between 6000 and 6500 b2k.

The Holocene core HM1 is correlated through the LST with the core AU2, which represents the time interval from the LST up to 60 000 b2k (Fig. 3). Generally, 88 flood layers over 7.5 mm occur in AU2 (Fig. 7 and Table 1). The LEZ 3 (10 500–14 700 b2k; boreal forest) has 20 flood layers and an average of 4.8 events per 1000 years. 12 strong flood events from 12 000 to 13 000 b2k represent the highest number of flood events per 1000 years in the whole time series of AU2 (Table 1) and is comparable to the Younger Dryas (McManus et al., 2004).

The late LEZ 4 (14 700–21 000 b2k, polar desert) reveals an average of 1.8 flood events per 1000 years and has 11 events in total. The Last Glacial Maximum (LGM) from 17 500 to 22 000 b2k shows no flood events at all; apparently it was so dry, that there was no spring snow melt during the peak glacial permafrost conditions. However, the summer temperatures each year, were high enough to break up the winter ice. There is no indication of event layers that could document perennial frozen ice on the maar lake. The succession of laminae appears to be almost continuous throughout the entire glaciation maximum (Sirocko et al., 2016–in this volume). The first suspension layers arise again at the time around 17 500 b2k (Table 1 and Fig. 8) and show, that the final phase of the Weichselian glaciation must have been already more humid than the LGM. Most

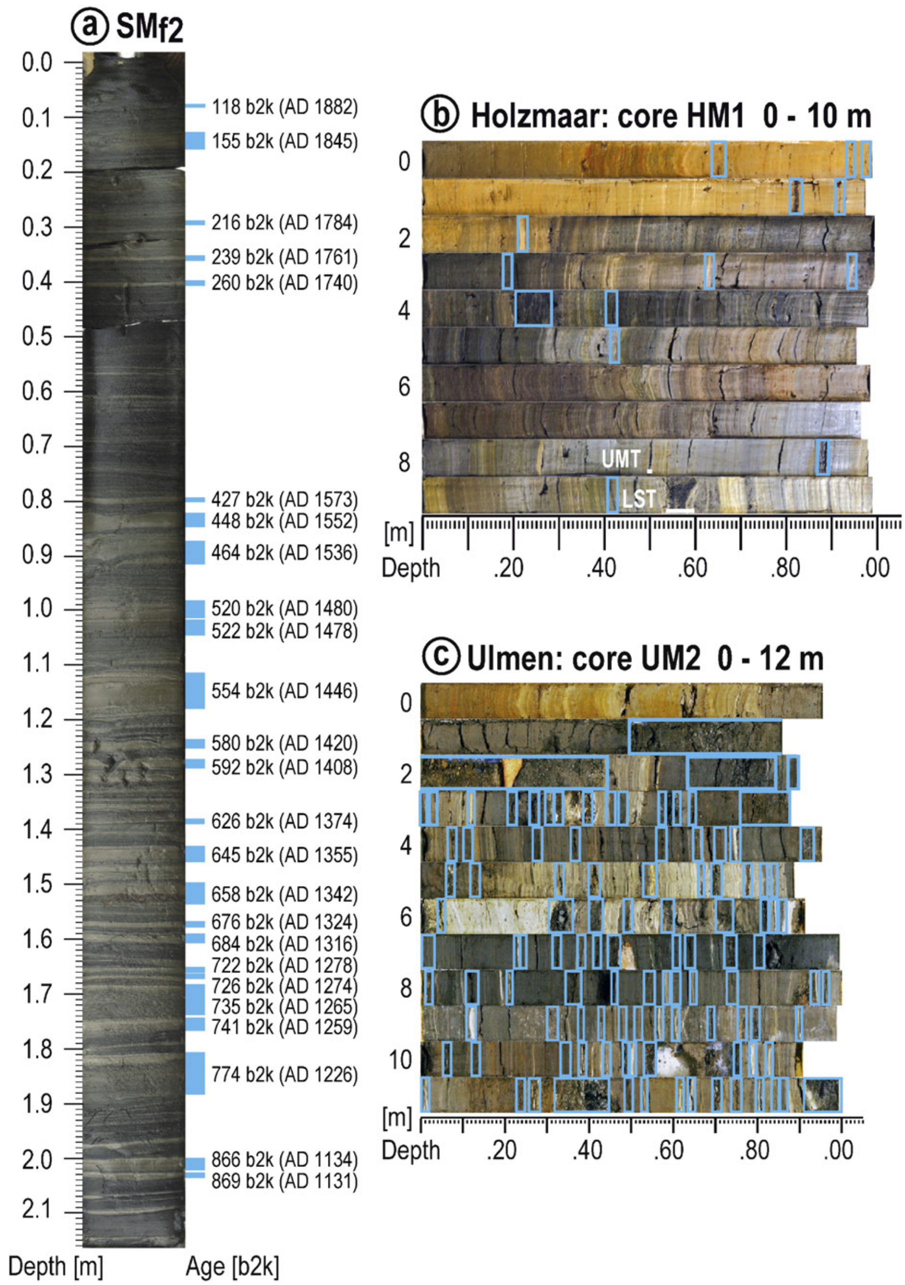

Fig. 6. a) Core SM_{f2} with all detected flood events (blue squares) and varve counted years. b) Core HM1 with all detected flood events (blue boxes) and tephra (white lines). c) Core UM2 with all detected flood events (blue boxes).

probably, the precipitation fell as winter snow, leading to spring meltwater runoff into the maar lakes.

The LEZ 5 (21 000–28 500 b2k, tundra) has 15 flood layers with an average of 1.8 flood events per 1000 years. Almost all flood events are restricted to the time period from 23 000 to 24 000 b2k, representing the end of Greenland Stadial 3 (Table 1 and Fig. 8).

The LEZ 6 (28 500–36 500 b2k; steppe) was a steppe environment and has seen an average of 4 flood events per 1000 years. The period shows a total of 34 flood events and thus, the highest number in the whole time series of AU2 (Table 1). The maximum flood cluster appears during the Greenland Stadial 5, particular during the transition from GI 5 to GI 4 (Table 1 and Fig. 8). The late winter snow melt events still seem to be the main causes for these flood events, indeed the occurrence of summer rains in a landscape with little vegetation cover might have lead to erosion even at moderate rainfall intensity. The occurrence of large amounts of Ranunculaceae seeds point towards quite humid conditions during summer (Sirocko et al., 2016–in this volume).

The LEZ 7 (36 500–49 000 b2k; boreal forest) has an average of 0.6 flood events per 1000 years and 8 events in total. Once again the flood events are concentrated in a short period of time from 44 000 to 44 500 b2k (Table 1 and Fig. 8). They occurred in a time when the boreal forest deteriorated into the subsequent steppe, (i.e. during a time of vegetation and soil change). This represents the Greenland Stadial 12 between GI 12 and GI 11.

Flood events are absent in LEZ 8 (49 000–55 000 b2k; spruce and hornbeam forest) and LEZ 9 (55 000–60 000 b2k; spruce forest), most probably since dense forests with roots stabilized the ground and no extreme precipitation events occurred (Table 1 and Fig. 8). On the other hand, it is very unlikely that flood events lacking in the entire warmer phase of the LEZ 8 and 9. It can be also explained by a missing

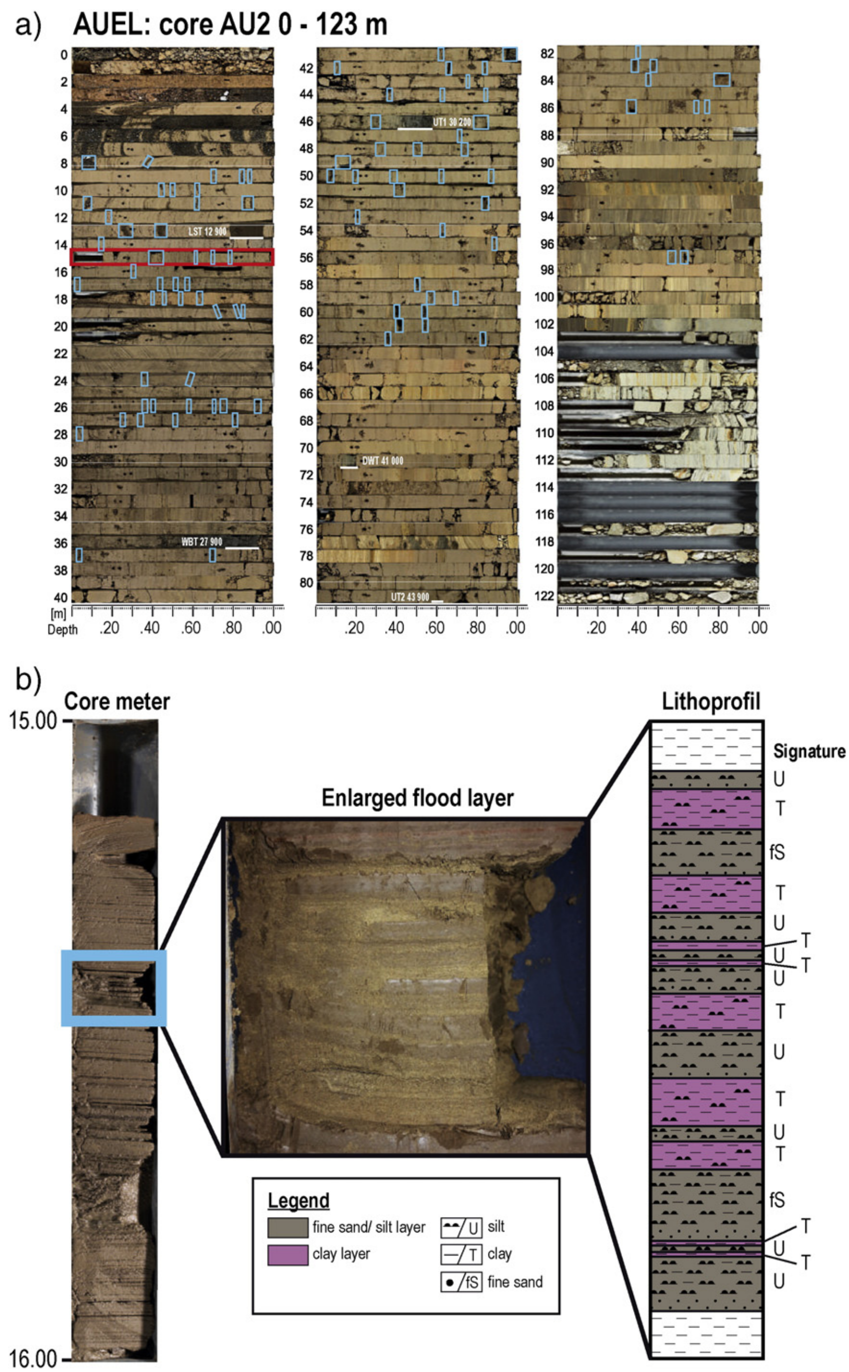

Fig. 7. a) Core AU2 with all detected flood events (blue boxes) and tephra (white lines). The first 7 m cannot be analysed due to the silting up and the strong anthropogenic impact. The core metres from 103 onwards counts to the eruption phase. The red core metre is the sample metre for Fig. 7b. b) Exemplary flood layer from the depth of 15.41 m. The enlarged flood layer and the lithoprofile show multiple water discharge peaks. Within the same flood event sand and silt layers, which represent water discharge peaks, alternate with clay sections.

connection between the young maar and the local river. Therefore, the sensitivity for flood events at this time was not given.

Summarized the main flood stages for AU2 are from 11 500 to 17 500, 23 000 to 24 000, 29 000 to 35 000 and 44 000 to 44 500 b2k (Table 1). However, the section from 11 500 to 17 500 b2k is the only one, which is spread over two LEZ zones. The period begins with the first snow melt events at the end of the polar desert phase, although the stage reaches the flood peak intensity around the Younger Dryas (Table 1 and Fig. 8). All three other flood stages are limited to one LEZ, whereby the phase from 29 000 to 35 000 b2k has a special position. Although it is with 6000 years the longest continuous phase with flood layers in the core AU2, there is a flood maximum from 29 000 to 32 000 b2k representing the Greenland Stadial 5 between the GI 5 and 4 (Fig. 8).

7. Discussion

The aim of this study is to analyse the variances of the flood frequency in central Europe and not to provide an absolute count of flood layers. The flood events are reconstructed from three Holocene maar lakes and one Pleistocene dry maar structure and thus, the data are not fully comparable. Therefore, the ELSA-Flood-Stack is a summary, which cannot be used as a direct precipitation curve. It can be understood as a reliable record of periods with extreme weather events or local to the Eifel. It is

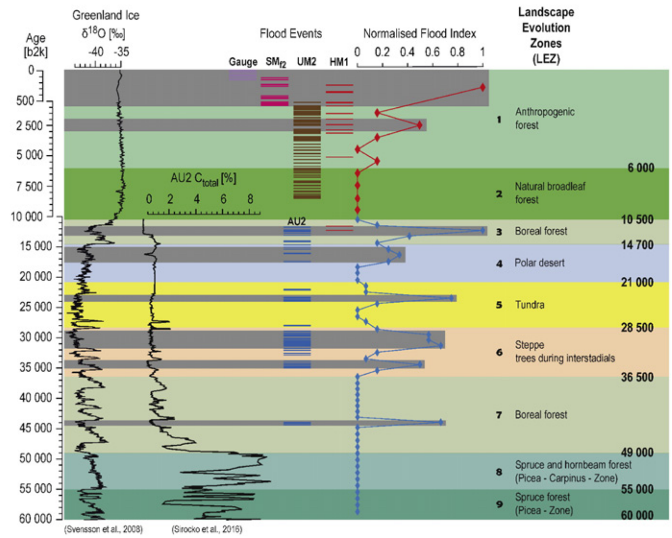

Fig. 8. The ELSA-Flood-Stack. Interaction between flood events (purple, pink, brown, red and blue lines), normalised flood index (red line represents HM1; blue line AU2) and LEZ subdivisions (Sirocko et al., 2016–in this volume). Additionally, the Greenland ice core isotopes time series (Svensson et al., 2008) and the Ctotal time series from Auel (Sirocko et al., 2016–in this volume) are shown.

obvious that the particles in flood layers are not solely associated to ephemeral precipitation and seasonal runoff. They are certainly affected by permafrost conditions, soil development and especially vegetation. A seasonal subdivision in summer and winter flood layers is currently not possible. Further analyses of pollen and diatoms are prime candidates to solve this problem. Nevertheless, the flood frequency of the Eifel indicates a trans-regional pattern and represents a climatic homogenous region from Belgium to Poland across Central Europe (Wernli and Pfahl, 2009). Varying offsets between flood events of rivers both in Germany and Europe have been described by Glaser (2008) and can be explained by the complex regional weather situation. In this context, a detailed comparison with the flood time series from Macklin et al., 2006; Zielhofer et al., 2008; Storen et al., 2010; Swierczynski et al., 2013; Wilhelm et al., 2013 and Wirth et al., 2013 will be subject of a future publication. Despite the complexity of the flood stack, it is possible to draw several conclusions about precipitation, flood frequency and related topics (Fig. 8).

The Picea-Zone (LEZ 9) and the Picea–Carpinus-Zone (LEZ 8) include the GI 17 up to GI 13 (see Fig. 8). Warm temperatures and sufficient rainfall were necessary for the spread of the relatively thermophilous forest. The soil stabilization as a result of increasing vegetation is mainly responsible for the reduction of fluvial sediment erosion. Nevertheless, a missing connection between the river and the young maar cannot be excluded at this time. Both possibilities explain the lack of flood layers in the LEZ 9 and 8 (Fig. 8).

During the climate change from GI 12 to GI 11, the vegetation passes into an open boreal coniferous forest with high proportions of grasses (Sirocko et al., 2016–in this volume). Through the withdrawal of forests and the increasing desertification of the landscape, the root penetration of the soil declines. The soil loses stability, so that heavy rain events could erode and easier rearrange the sediments. This process is confirmed by several flood layers in the period from 44 500 to 44 000 b2k (Fig. 8).

The evolution from a boreal forest to an almost treeless steppe took place at the end of the LEZ 7 (GI 8). Thus, occasional rain and snow melt events could easily erode the soil. Therefore, this steppe phase is characterized by continuous flood events with a maximum during the climate change after the GI 5 (Fig. 8).

The LEZ 5 is characterized by a vegetation decrease as a result of reduced temperatures and low precipitation rates. However, a bigger cluster of flood events could be identified at the time interval from 24 000 to 23 000 b2k and display the end of Greenland Stadial 3 (Fig. 8).

After 21 000 b2k, the landscape in the Eifel turned into an ice desert and represents the last glacial maximum (22 000–17 500 b2k). The first flood layers appear again at the time around 17 500 b2k when the first snow melt events start. Due to the lack of vegetation, the high potential of soil erosion leads to several flood layers. The slightly moister climate combined with only gradually increasing vegetation density induces a large number of flood layers in the LEZ 3 (Fig. 8). Especially the Younger Dryas cold event stands out with a high number of flood events. A detailed consideration of the short transitional period from the cores HM1 and AU2 allows further conclusions. Due to the fact that the river just touches lake Holzmaar, only extreme flood events are preserved. In contrast, the Aueler Maar is very sensitive for flood deposits, since the river flows directly through the maar center. While in Auel 14 flood layers have been identified only two flood layers are classified in Holzmaar. Thus, the Younger Dryas cold event is characterized by a large amount of flood events, where only a few have the potential for a millennium flood.

After the Younger Dryas, the late glacial boreal forest transforms quickly into a thermophilic forest. The early Holocene forests reduce the building of flood layers despite high rainfall, thus, flood layers occur not as pronounced as during LEZ 3 (Fig. 8). Nevertheless, a slight flood cluster arises between 6500 and 6000 b2k. This period confirms new evidences on a mid-Holocene climatic depression with elevated flood activity (Macklin et al., 2006; Magny et al., 2007 and Zielhofer et al., 2008).

The beginning of the LEZ 1 was described as a shift to a more humid and cooler climate (Firbas, 1949 and Overbeck, 1975). Especially after 4000 b2k the number of flood layers increase rapidly in all cores (Fig. 8). The pollen analysis indicates a strong anthropogenic influence, as a result of forest clearing and agricultural activities. The growing population of the Bronze Age results in rising soil erosion, which is reflected in the Holocene river activity from Germany (Hoffmann et al., 2008). The period after 4000 b2k shows the highest flood activity at all, although it is the only flood stage which belongs to a warm phase. The increase of the flood frequency is therefore a combination between higher amounts of precipitation and in particular the human impact.

8. Conclusions

The understanding of magnitudes and frequencies of flood events are still limited, although they are one of the most important natural hazards in the world. Flood layers in maar sediments represent an environmental history based on individual events. Consequently, flood layers provide a proxy archive with unique environmental information, depending on local conditions like vegetation and permafrost. Our time-series from the Eifel represents the first highly-resolved flood frequency record for the last 60 000 years and indicates variable periodicities of flood activity linked to predominant climatic and anthropogenic development. The maximum flood phases in the Eifel reflect regional and global climate fluctuations. They are clustered in the periods from 11 500 to 17 500 (late glacial and Younger Dryas), 23 000 to 24 000 (before GI 2), 29 000 to 35 000 (especially between GI 5 and 4) and 44 000 to 44 500 b2k (transition from GI 12 to 11). Summarized, episodes with high frequencies of extreme flood events were found to be associated with periods of cool and wet climate, whereas episodes with low frequencies of extreme floods were related to periods of warm and constant climate. However, during the late Holocene land use related to the human impact has been the main trigger for the increase of flood events. It turns out that low vegetation coverage related to Greenland Stadial phases or anthropogenic impact are the main causes for the development of flood layers in maar sediments, while precipitation plays only a secondary role. This interpretation of our data is consistent

Table 1
Time overview of all flood events from the gauge analysis and the core SMf2, as well as the number of flood events per 1000 years from the cores HM1, UM2 and AU2.

Gauge	Gauge	SMf2	SMf2	Time interval	HM1	UM2	AU2
[b2k]	[AD]	[b2k]	[AD]	[b2k]	[n per 1000 a]	[n per 1000 a]	[n per 1000 a]
5	1995	118	1882	1 – 1000	6	10	
7	1993	155	1845	1001 – 2000	1	20	
12	1988	216	1784	2001 – 3000	3	13	
52	1948	239	1761	3001 – 4000	1	15	
74	1926	260	1740	4001 – 5000	0	8	
80	1920	427	1573	5001 – 6000	1	5	
118	1882	448	1552	6001 – 7000	0	13	
155	1845	464	1536	7001 – 8000	0	11	
		520	1480	8001 – 9000	0	10	
		522	1478	9001 – 10 000	0		
		554	1446	10 001 – 11 000	0		
		580	1420	11 001 – 12 000	1		2
		592	1408	12 001 – 13 000	1		12
		626	1374	13 001 – 14 000			5
		645	1355	14 001 – 15 000			2
		658	1342	15 001 – 16 000			3
		676	1324	16 001 – 17 000			4
		684	1316	17 001 – 18 000			3
		722	1278	18 001 – 19 000			0
		726	1274	19 001 – 20 000			0
		735	1265	20 001 – 21 000			0
		741	1259	21 001 – 22 000			1
		774	1226	22 001 – 23 000			1
		866	1134	23 001 – 24 000			9
		869	1131	24 001 – 25 000			2
				25 001 – 26 000			0
				26 001 – 27 000			0
				27 001 – 28 000			1
				28 001 – 29 000			2
				29 001 – 30 000			7
				30 001 – 31 000			7
				31 001 – 32 000			8
				32 001 – 33 000			2
				33 001 – 34 000			1
				34 001 – 35 000			6
				35 001 – 36 000			2
				36 001 – 37 000			0
				37 001 – 38 000			0
				38 001 – 39 000			0
				39 001 – 40 000			0
				40 001 – 41 000			0
				41 001 – 42 000			0
				42 001 – 43 000			0
				43 001 – 44 000			0
				44 001 – 45 000			8
				45 001 – 46 000			0
				46 001 – 47 000			0
				47 001 – 48 000			0
				48 001 – 49 000			0
				49 001 – 50 000			0
				50 001 – 51 000			0
				51 001 – 52 000			0
				52 001 – 53 000			0
				53 001 – 54 000			0
				54 001 – 55 000			0
				55 001 – 56 000			0
				56 001 – 57 000			0
				57 001 – 58 000			0
				58 001 – 59 000			0
				59 001 – 60 000			0

with several studies of fluvial erosion related to vegetation coverage (Mol (1997); Macklin et al., 2002; Vandenberghe (2003).

Supplementary data to this article can be found online at http://dx.doi.org/10.1016/j.gloplacha.2015.12.003.

Acknowledgments

This work is financed by the German Science Foundation (DFG) and part of the ELSA-Project (Eifel Laminated Sediment Archive Project). Carsten Costard did the photographing of the sediment cores and Petra Sigl supported the creation of the images. Furthermore, we are grateful to the State Office for Environment, Water Management and Trade Control Rhineland-Palatinate for providing the gauge data sets of the Eifel rivers and the Federal Institute of Hydrology for the gauge data sets of the rivers Moselle and Rhine. The authors thank the anonymous reviewer for the constructive comments that help to improve the quality of this manuscript. At last we would like to thank Frank Dreher, Hilmar Holland, Klaus Schwibus, Sabine Hahn and Saskia Rudert for their assistance.

References

Ampel, L., Wohlfarth, B., Risberg, J., Veres, D., 2008. Paleolimnological response to millennial and centennial scale climate variability during MIS 3 and 2 as suggested by the diatom record in Les Echets, France. Quat. Sci. Rev. 27, 1493–1504.

Andersen, K.K., Svensson, A., Johnsen, S.J., Rasmussen, S.O., Bigler, M., Röthlisberger, R., Ruth, U., Siggaard-Andersen, M.-L., Steffensen, M.B., Dahl-Jensen, D., Vinther, B.M., Clausen, H.B., 2006. The Greenland ice core chronology 2005, 15–42 ka. Part 1: constructing the time scale. Quat. Sci. Rev. 25, 3246–3257.

Anselmetti, F.S., Artiztegui, D., De Batist, M., Gebhardt, A.C., Haberzettl, T., Niessen, F., Ohlendorf, C., Zolitschka, B., 2009. Environmental history of southern Patagonia unravelled by the seismic stratigraphy of Laguna Potrok Aike. Sedimentology 56, 873–892.

Bork, H.R., Bork, H., Dalchow, C., Faust, B., Piorr, H.P., Schatz, T., 1998. Landschaftsentwicklung in Mitteleuropa. Klett-Perthes, Gotha/Stuttgart.

Bouma, A.H., 1987. Megaturbidite: an acceptable term? Geo-Mar. Lett. 7, 63–67.

Brauer, A., 1994. Weichselzeitliche Sedimente des Holzmaares – Warvenchronologie des Hochglazials und Nachweis von Klimaschwankungen. Doc. Nat. 85, 1–210.

Brauer, A., Endres, C., Negendank, J.F.W., 1999a. Lateglacial calendar year chronology based on annually laminated sediments from Lake Meerfelder Maar. Germany. Quat. Int. 61.

Brauer, A., Endres, C., Günter, C., Litt, T., Stebich, M., Negendank, J.F., 1999b. High resolution sediment and vegetation responses to Younger Dryas climate change in varved lake sediments from Meerfelder Maar, Germany. Quat. Sci. Rev. 18, 321–329.

Brauer, A., Mingram, J., Frank, U., Günter, C., Schettler, G., Wulf, S., Zolitschka, B., Negendank, J.F.W., 2000. Abrupt environmental oscillations during the Early Weichselian recorded at Lago Grande di Monticchio, southern Italy. Quat. Int. 73, 79–90.

Brauer, A., Litt, T., Negendank, J.F.W., Zolitschka, B., 2001. Lateglacial varve chronology and biostratigraphy of lakes Holzmaar and Meerfelder Maar. Germany, BOREAS 30, 83–88.

Brakenridge, G.R., Thomas, P.A., Conkey, L.E., Schiferle, J.C., 1988. Fluvial sedimentation in response to postglacial uplift and environmental change, Missisquoi River. Vermont. Quatern. Res. 30, 190–220.

Büchel, G., 1993. Maars of the Westeifel, Germany: Paleolimnology of European maar lakes. Springer, Berlin, Heidelberg (Ch.1).

Dyck, S., Peschke, G., 1995. Grundlagen der Hydrologie. Verlag Bauwesen.

Federal Waterways and Shipping Administration, 2015. (WSV) provided by the German Federal Institute of Hydrology (BfG): Daily Gauge Values, Moselle, Cochem 1963–2013; Daily Gauge Values, Moselle, Trier 1966–2013; Daily Gauge Values, Rhine, Koblenz 1955–2013; Daily Gauge Values, Rhine, Bonn 1920–2013; Daily Gauge Values, Rhine, Cologne 1900–2013.

Firbas, F., 1949. Spät- und nacheiszeitliche Waldgeschichte Mitteleuropas nördlich der Alpen. Band 1 und 2. Gustav Fischer Verlag, Jena.

Förster, M.W., Sirocko, F., 2016. Volcanic activity in the Eifel during the last 500,000 years: The ELSA-Tephra-Stack. Glob. Planet. Chang. 142, 100–107 (in this volume).

Glaser, R., 2008. Klimageschichte Mitteleuropas. 1200 Jahre Wetter, Klima, Katastrophen. Mit Prognosen für das 21. Jahrhundert. Wissenschaftliche Buchgesellschaft, Darmstadt.

Gronenborn, D., Sirocko, F., 2009. 4400–3400 BC Viehwirtschaft und Ausbreitung der Michelsberger Kultur. In: Sirocko, F. (Ed.), Wetter - Klima - Menschheitsentwicklung. Von der Eiszeit bis ins 21. Jahrhundert. Theiss Verlag.

Hajdas, I., Zolitschka, B., Ivy-Ochs, S.D., Beer, J., Bonani, G., Leroy, S.A.G., Negendank, J.W., Ramrath, M., Suter, M., 1995. AMS radiocarbon dating of annually laminated sediments from Lake Holzmaar, Germany. Quat. Sci. Rev. 14, 137–143.

Hoffmann, T., Lang, A., Dikau, R., 2008. Holocene river activity: analysing 14C-dated fluvial and colluvial sediments from Germany. Quat. Sci. Rev. 27, 2031–2040.

IPCC, 2014. Climate Change 2014: Synthesis Report. Contribution of Working Groups I, II and III to the Fifth Assessment Report of the Intergovernmental Panel on Climate Change.

IPCC, 2007. Climate Change 2007: Synthesis Report. Contribution of Working Groups I, II and III to the Fourth Assessment Report of the Intergovernmental Panel on Climate Change.

Jacob, D., Bärring, L., Christensen, O.B., Christensen, J.H., Hagemann, S., Hirschi, M., Kjellström, E., Lenderink, G., Rockel, B., Schär, C., Seneviratne, S.I., Somot, S., van Ulden, A., van den Hurk, B., 2007. An inter-comparison of regional climate models for Europe: Design of the experiments and model performance. Clim. Chang. 81, 31–52.

Kämpf, L., Brauer, A., Swierczynski, T., Czymzik, M., Müller, P., Dulski, P., 2014. Processes of flood-triggered detrital layer deposition in the varved Lake Mondsee sediment record revealed by a dual calibration approach. J. Quat. Sci. 29, 475–486.

Marco, S., Stein, M., Agnon, A., Ron, H., 1996. Long-term earthquake clustering: A 50,000-year paleoseismic record in the Dead Sea Graben. J. Geophys. Res. 101, 6179–6191.

Macklin, M.G., 1999. Holocene river environments in prehistoric Britain: human interaction and impact. J. Quat. Sci. 14, 521–530.

Macklin, M.G., Benito, G., Gregory, K.J., Johnstone, E., Lewin, J., Michczyńska, D.J., Soja, R., Starkel, L., Thorndycraft, V.R., 2006. Past hydrological events reflected in the Holocene fluvial record of Europe. *Catena*Elsevier.

Macklin, M.G., Fuller, I.C., Lewin, J., Maas, G.S., Passmore, D.G., Rose, J., Woodward, J.C., Black, S., Hamlin, R.H.B., Rowan, J.S., 2002. Correlation of fluvial sequences in the Mediterranean basin over the last 200 ka and their relationship to climate change. Quat. Sci. Rev. 21, 1633–1641.

Magny, M., de Beaulieu, J.L., Drescher-Schneider, R., Vanniere, B., Walter-Simonnet, A.V., Miras, Y., Millet, L., Bossuet, G., Peyron, O., Brugiapaglia, E., Leroux, A., 2007. Holocene climate changes in the central Mediterranean as recorded by lake-level fluctuations at Lake Accesa (Tuscany, Italy). Quat. Sci. Rev. 26, 1736–1758.

McManus, J.F., Francois, R., Gherardi, J.M., Keigwin, L.D., Brown-Leger, S., 2004. Collapse and rapid resumption of Atlantic meridional circulation linked to deglacial climate changes. Nature 428, 834–837.

Mol, J., 1997. Fluvial response to Weichselian climate changes in the Niederlausitz (Germany). J. Quat. Sci. 12, 43–60.

Moreno, A., Valero-Garces, B., Gonzales-Samperiz, P., Rico, M., 2008. Flood response to rainfall variability during the last 2000 years inferred from the Taravilla Lake record (Central Iberian Range, Spain). J. Paleolimnol. 40, 943–961.

Moschen, R., 2004. Die Sauerstoffisotopenverhältnisse des biogenen Opals lakustriner Sedimente als mögliches Paläothermometer (Diplomathesis) Universität Köln, Germany.

Mulder, T., Alexander, J., 2001. The physical character of subaqueous sedimentary density flows and their deposits. Sedimentology 48, 269–299.

Mulder, T., Syvitski, J.P.M., Migeon, S., Faugères, J.-C., Savoye, B., 2003. Marine hyperpycnal flows: initiation, behavior and related deposits. A review. Mar. Pet. Geol. 20, 861–882.

Municipal drainage operations of Cologne, Flood Protection Centre. www.steb-koeln.de (20.01.) .

Nardin, T.R., 1979. A review of mass movement processes sediment and acoustic characteristics, and contrasts in slope and base-of-slope systems versus canyon-fan-basin floor systems. Soc. Econ. Paleontol. Mineral. 27, 61–73.

Overbeck, F., 1975. Botanisch-Geologische Moorkunde. Karl Wachholtz Verlag, Neumünster, pp. 145–154 (Past 6).

Scharf, B.W., Oehms, M., 1992. Physical and chemical characteristics. Limnology of Eifel Maar Lakes. Ergebnisse der Limnologie 38, pp. 63–83.

Schlolaut, G., Brauer, A., Marshall, M.H., Nakagawa, T., Staff, R.A., Bronk Ramsey, C., Lamb, H.F., Bryant, C.L., Naumann, R., Dulski, P., Brock, F., Yokoyama, Y., Tada, R., Haraguchi, T., Suigetsu 2006 Project members, 2014. Event layers in the Japanese Lake Suigetsu 'SG06' sediment core: description, interpretation and climatic implications. Quat. Sci. Rev. 83, 157–170.

Schnellmann, M., Anselmetti, F.S., Giardini, D., McKENZIE, J.A., 2005. Mass movement-induced fold-and-thrust belt structures in unconsolidated sediments in Lake Lucerne (Switzerland). Sedimentology 52, 271–289.

Seelos, K., Sirocko, F., 2005. RADIUS–rapid particle analysis of digital images by ultra-high-resolution scanning of thin sections. Sedimentology 52, 669–681.

Sirocko, F., 2009. Wetter - Klima - Menschheitsentwicklung. Von der Eiszeit bis ins 21. Jahrhundert. Theiss Verlag., p. 208.

Sirocko, F., Dietrich, S., 2009. Wetter - Klima - Menschheitsentwicklung. Von der Eiszeit bis ins 21. Jahrhundert. Theiss Verlag (Chapter 4).

Sirocko, F., Dietrich, S., Veres, D., Grootes, P., Schaber-Mohr, K., Seelos, K., Nadeau, M.-J., Kromer, B., Rothacker, L., Röhner, M., Krbetschek, M., Appleby, P., Hambach, U., Rolf, C., Sudo, M., Grim, S., 2013. Multi-Proxy-Dating of Holocene maar lakes and Pleistocene dry maar sediments in the Eifel, Germany. Quat. Sci. Rev. 62, 56–72.

Sirocko, F., Knapp, H., Dreher, F., Förster, M.W., Albert, J., Brunck, H., Veres, D., Dietrich, S., Zech, M., Hambach, U., Röhner, M., Rudert, S., Schwibus, K., Adams, C., Sigl, P., 2016. The ELSA-Vegetation-Stack: Reconstruction of Landscape Evolution of the last 60 000 years. Glob. Planet. Chang. 142, 108–135 (in this volume).

Sirocko, F., Seelos, K., Schaber, K., Rein, B., Dreher, F., Diehl, M., Lehne, R., Jäger, K., Krbetschek, M., Degering, D., 2005. A late Eemian aridity pulse in central Europe during the last glacial inception. Nature 436, 833–836.

State Office for Environment, Water Management and Trade Control Rhineland-Palatinate, 2015. (LUWG): Daily Gauge Values, Ahr, Altenahr 1945–2014; Daily Gauge Values, Kyll, Densborn 1972–2014; Daily Gauge Values, Prüm, Prümzurlay 1972–2014.

Storen, E.N., Dahl, S.O., Nesje, A., Paasche, Ø., 2010. Identifying the sedimentary imprint of high-frequency Holocene river floods in lake sediments: development and application of a new method. Quat. Sci. Rev. 29, 3021–3033.

Straka, H., 1975. Die spätquartäre Vegetationsgeschichte der Vulkaneifel. Beiträge zur Landespflege in Rheinlandpfalz 3, pp. 1–163.

Sturm, M., Siegenthaler, C., Pickrill, R.A., 1995. Turbidites and homogenites — a conceptual model of flood and slide deposits. Publication of IAS- 16th regional meeting sedimentology, Paris, p. 22.

Svensson, A., Andersen, K.K., Bigler, M., Clausen, H.B., Dahl-Jensen, D., Davies, S.M., Johnsen, S.J., Muscheler, R., Parrenin, F., Rasmussen, S.O., Röthlisberger, R., Seierstad, I., Steffensen, J.P., Vinther, B.M., 2008. A 60 000 year Greenland stratigraphic ice core chronology. Clim. Past 4, 47–57.

Swierczynski, T., Lauterbach, S., Dulski, P., Delgado, J., Merz, B., Brauer, A., 2013. Mid-to late Holocene flood frequency changes in the northeastern Alps as recorded in varved sediments of Lake Mondsee (Upper Austria). Quat. Sci. Rev. 80, 78–90.

Thorndycraft, V.R., Benito, G., Rico, M., Sopeña, A., Sánchez-Moya, Y., Casas, A., 2005. A long-term flood discharge record derived from slackwater flood deposits of the Llobregat River, NE Spain. J. Hydrol. 313, 16–31.

Vandenberghe, J., 2003. Climate forcing of fluvial system development: an evolution of ideas. Quat. Sci. Rev. 22, 2053–2060.

Walker, R.G., Mutti, E., 1973. Part IV. Turbidite Facies and Facies Associations. Turbidites and Deep Water Sedimentation, 119–158. Water management administration Rhineland-Palatinate, German river code 266374.

Wernli, H., Pfahl, S., 2009. Grundlage des Klimas und extremer Wettersituationen. Wetter, Klima, Menschheitsentwicklung. Von der Eiszeit bis ins 21. Jahrhundert. Theiss, Stuttgart, pp. 44–52.

Wessels, M., 1998. Natural environmental changes indicated by Late Glacial and Holocene sediments from Lake Constance, Germany. Palaeogeogr. Palaeoclimatol. Palaeoecol. 140, 421–432.

Wilhelm, B., Arnaud, F., Enters, D., Allignol, F., Legaz, A., Magand, O., Revillon, S., Giguet-Covex, C., Malet, E., 2012a. Does global warming favour the occurrence of extreme floods in European Alps? First evidences from a NW Alps proglacial lake sediment record. Clim. Chang. 113, 563–581.

Wilhelm, B., Arnaud, F., Sabatier, P., Crouzet, C., Brisset, E., Chaumillon, E., Disnar, J.-R., Guiter, F., Malet, E., Reyss, J.-L., Tachikawa, K., Bard, E., Delannoy, J.-J., 2012b. 1400 years of extreme precipitation patterns over the Mediterranean French Alps and possible forcing mechanisms. Quat. Res. 78, 1–12.

Wilhelm, B., Arnaud, F., Sabatier, P., Magand, O., Chapron, E., Courp, T., Tachikawa, K., Fanget, B., Malet, E., Pignol, C., Bard, E., Delannoy, J.-J., 2013. Palaeoflood activity and climate change over the last 1400 years recorded by lake sediments in the north-west European Alps. J. Quat. Sci. 28, 189–199.

Wirth, S.B., Girardclos, S., Rellstab, C., Anselmetti, F.S., 2011. The sedimentary response to a pioneer geo-engineering project: Tracking the Kander River deviation in the sediments of Lake Thun (Switzerland). Sedimentology 58, 1737–1761.

Wirth, S.B., Glur, L., Gilli, A., Anselmetti, F.S., 2013. Holocene flood frequency across the Central Alps—solar forcing and evidence for variations in North Atlantic atmospheric circulation. Quat. Sci. Rev. 80, 112–128.

Wohlfarth, B., Veres, D., Ampel, L., Lacourse, T., Blaauw, M., Preusser, F., Andrieu-Ponel, V., Kéravis, D., Lallier-Vergès, E., Björck, S., Davies, S., de Beaulieu, J.-L., Risberg, J., Hormes, A., Kasper, H.U., Possnert, G., Reille, M., Thouveny, N., Zander, A., 2008. Rapid ecosystem response to abrupt climate changes during the last glacial period in western Europe, 40–16 ka. Geology 36, 407–410.

Zielhofer, C., Faust, D., Linstädter, J., 2008. Late Pleistocene and Holocene alluvial archives in the Southwestern Mediterranean: Changes in fluvial dynamics and past human response. Quaternary International. Elsevier.

Zolitschka, B., 1998. Paläoklimatische Bedeutung laminierter Sedimente. Gebrüder Borntäger, Berlin, Stuttgart.

Zolitschka, B., Negendank, J.F.W., Lottermoser, B.G., 1995. Sedimentological proof and dating of the Early Holocene volcanic eruption of Ulmener Maar. Geol. Rundsch. 84, 213–219.